
Effective Medium Theory for Drag Reducing Micro-patterned Surfaces in Turbulent Flows

ILENIA BATTIATO¹

¹ *Mechanical Engineering Department, Clemson University - Clemson, SC, 29634*

PACS 47.56.+r – Fluid flow through porous media
PACS 83.50.Rp – Slip flows and wall slip
PACS 47.60.-i – Flow in quasi-one-dimensional systems

Abstract – Inspired by the *lotus effect*, many studies in the last decade have focused on micro- and nano-patterned surfaces. They revealed that patterns at the micro-scale combined with high contact angles can significantly reduce skin drag. However, the mechanisms and parameters that control drag reduction, e.g. Reynolds number and pattern geometry, are still unclear. We propose an effective medium representation of the micro-features, that treats the latter as a porous medium, and provides a framework to model flow over patterned surfaces in both Cassie and Wenzel states. Our key result is a closed-form expression for the skin friction coefficient in terms of frictional Reynolds (or Kármán) number in turbulent regime, the viscosity ratio between the fluid in and above the features, and their geometrical properties. We apply the proposed model to turbulent flows over superhydrophobic ridged surfaces. The model predictions agree with laboratory experiments for Reynolds numbers ranging from 3000 to 10000.

Introduction. – The *lotus effect* has recently entered the scientific jargon to refer to superhydrophobicity. One of the necessary ingredients for a surface to be superhydrophobic is the presence of nano- and micro-scale features. Patterned surfaces have shown drag-reducing abilities in both laminar [1–5] and turbulent [6, 7] regimes, and in either Cassie [6] or Wenzel (or fakir) state [2–4]. The former is characterised by the fluid impregnating the textured surface, while in the latter the liquid interface is suspended on an air cushion above the roughness peaks.

Drag reduction in turbulent flows by means of micropatterned superhydrophobic surfaces is of crucial importance because of its profound effects on a number of existing technologies. Yet, the optimal design of nano- and micro-scale roughness/structures for turbulent drag reduction is hampered by the relative lack of quantitative understanding of their impact on macroscopic flow observables, such as skin friction coefficient and slip length. Also, the impact of Reynolds number is unclear, and the upper limit of superhydrophobic drag reduction is still unknown [8]. Attempts to relate geometrical properties of the micro-features to macroscopic quantities, e.g. slip length, are mainly phenomenological [4], and analytical expressions are available only for tractable geometries [9, 10]. Thus, a suitable framework able to quantify effective properties of

such surfaces and their connection to microscopic features is still needed [11].

In this work we propose an effective-medium representation of Cassie- and Wenzel-like textured surfaces in turbulent flows. We develop closed-form expressions for the skin friction coefficient in terms of the geometrical properties of the patten and the friction Reynolds (or Kármán) number. This is accomplished by treating the features as a porous medium. The Reynolds equation for fully turbulent channel flow over the pattern is coupled to the porous media Brinkman equation for flow through the roughness. We test the model veracity by comparing our closed-form expressions with skin friction data of turbulent channel flows over superhydrophobic grooved surfaces for Reynolds number ranging from 3000 to 10000 [7].

Model Formulation. – We consider pressure-driven channel flow through, $\hat{y} \in (-H, 0)$, and over, $\hat{y} \in (0, 2L)$, an array of micro-ridges. Following [12, 13], we treat the micro-patterned surface as a porous medium with permeability K , and couple Brinkman and Reynolds equations to describe a distribution of the horizontal component of the average velocity $\hat{u}(\hat{y})$ through, $\hat{y} \in (-H, 0)$, and above

the pattern, $\hat{y} \in (0, 2L)$:

$$\mu_e d_{\hat{y}\hat{y}} \hat{u} - \mu_e K^{-1} \hat{u} - d_{\hat{x}} \hat{p} = 0, \quad \hat{y} \in (-H, 0) \quad (1a)$$

$$\mu d_{\hat{y}\hat{y}} \hat{u} - d_{\hat{y}} \langle \hat{u}' \hat{v}' \rangle - d_{\hat{x}} \hat{p} = 0, \quad \hat{y} \in (0, 2L) \quad (1b)$$

where μ_e and μ are the dynamic viscosities of the fluids inside and above the porous medium (i.e. grooved surface), respectively. In the turbulent regime, $d_{\hat{x}} \hat{p} < 0$ is an externally imposed mean pressure gradient, $\hat{\mathbf{u}} = [\hat{u}, \hat{v}]$ denotes the mean velocity, \hat{u}' and \hat{v}' are the velocity fluctuations about their respective means, and $\langle \hat{u}' \hat{v}' \rangle$ is the Reynolds stress. Fully-developed turbulent channel flow has velocity statistics that depend on \hat{y} only. No-slip is imposed at $\hat{y} = -H$ and $\hat{y} = 2L$. The formulation of appropriate boundary conditions at the interface between free and filtration (porous media) flows is still subject to open debate, which stems from the dispute of whether tangential velocity and shear stress at the interface are continuous or discontinuous [14–18]. Following [12, 13, 17] and many others, we impose the continuity of both velocity and shear stress at the interface, $\hat{y} = 0$. Such conditions have proven to provide accurate description of the macroscopic response of systems at the nanoscale [12, 13, 17]. Hence, eq. (1) are subject to

$$\begin{aligned} \hat{u}(-H) = 0, \quad \hat{u}(2L) = 0, \\ \hat{u}(0^-) = \hat{u}(0^+) = \hat{U}, \quad \mu_e d_{\hat{y}} \hat{u}|_{0^-} = \mu d_{\hat{y}} \hat{u}|_{0^+}, \end{aligned} \quad (2)$$

where \hat{U} is an unknown (slip) velocity at the interface $\hat{y} = 0$.

Choosing (L, μ, q) as repeating variables, with $q = -L^2 d_{\hat{x}} \hat{p} / \mu$ a characteristic velocity, eq. (1) can be cast in dimensionless form

$$M d_{yy} u - M \lambda^2 u + 1 = 0, \quad y \in (-\delta, 0) \quad (3a)$$

$$d_{yy} u - Re_\tau^2 d_y \langle u' v' \rangle + 1 = 0, \quad y \in (0, 2) \quad (3b)$$

subject to $u(-\delta) = 0$, $u(2) = 0$, $u(0^-) = u(0^+) = U$, and $M d_y u|_{0^-} = d_y u|_{0^+}$, where $y = \hat{y}/L$, $\delta = H/L$, $M = \mu_e/\mu$, $u = \hat{u}/q$, and $U = \hat{U}/q$. The parameter $\lambda^2 = (MK)^{-1} L^2$ is inversely proportional to dimensionless permeability, K/L^2 . The limit $\lambda \rightarrow \infty$ corresponds to the diminishing flow through the patterns due to decreasing permeability K . Furthermore, the Kármán (or frictional Reynolds) number, Re_τ , is defined as the Reynolds number based on the channel half-width and the skin-friction velocity $\hat{u}_\tau = (-L d_{\hat{x}} \hat{p} / \rho)^{1/2}$:

$$Re_\tau := \hat{u}_\tau L / \nu, \quad \text{or equivalently} \quad Re_\tau = (qL/\nu)^{1/2}, \quad (4)$$

and it determines the relative importance of viscous and turbulent processes. Assuming the surface of the porous medium is hydrodynamically smooth, the law of the wall imposes $d_y u|_{0^+} = 1$ since $u(y \rightarrow 0^+) = y + U$ in the viscous sublayer [13]. Therefore, inside the porous medium, i.e. $y \in [-\delta, 0]$, the solution for the dimensionless velocity

distribution $u(y)$ is given by

$$u(y) = (M\lambda^2)^{-1} + C_1 e^{\lambda y} + C_2 e^{-\lambda y}, \quad (5a)$$

$$C_{1,2} = \pm \frac{1}{M\lambda^2} \frac{(M\lambda^2 U - 1) e^{\pm \delta \lambda} + 1}{e^{\delta \lambda} - e^{-\delta \lambda}}, \quad (5b)$$

$$U = (M\lambda^2)^{-1} (1 + \lambda \tanh \delta \lambda - \text{sech} \delta \lambda). \quad (5c)$$

The skin friction coefficient is defined as $C_f = 2\hat{\tau}_0 / (\rho \hat{u}_b^2)$, where $\hat{\tau}_0 = \mu d_{\hat{y}} \hat{u}|_{0^+}$ is the shear stress at the edge of the pattern, $\hat{u}_b = q\chi$ is the average flow velocity, and $\chi = (2 + \delta)^{-1} \int_{-\delta}^2 u(y) dy$ is a dimensionless bulk velocity. From (4),

$$q = \frac{\nu Re_\tau^2}{L}. \quad (6)$$

Then, $\hat{u}_b = \nu Re_\tau^2 \chi / L$ and the skin friction coefficient is written in terms of Re_τ ,

$$C_f(Re_\tau) = \frac{2}{Re_\tau^2 \chi^2} \quad (7)$$

since $d_y u|_{0^+} = 1$. The dimensionless bulk velocity χ is rearranged as follows,

$$\chi = \frac{\chi_\delta + 2\chi_t}{2 + \delta}, \quad \chi_\delta = \int_{-\delta}^0 u(y) dy, \quad \chi_t = \frac{1}{2} \int_0^2 u(y) dy. \quad (8)$$

Equation (8) shows the impact of the pattern on the skin friction coefficient: $\chi \equiv \chi_t$ when $\delta = 0$, i.e. for a smooth channel. Integrating (5a), and combining the result with (5b) and (5c), we obtain

$$\chi_\delta = (M\lambda^3)^{-1} [\lambda(1 + \delta) + \text{sech} \Lambda (\text{csch} \Lambda - \lambda) - \coth \Lambda], \quad (9)$$

with $\Lambda = \lambda\delta$. The scale parameter Λ provides a formal classification between thin ($\Lambda \ll 1$) and thick ($\Lambda \gg 1$) porous media [13]. Since the pattern vertical length scale is generally very small compared to the height of the channel, i.e. $\delta \rightarrow 0$, we look for the asymptotic behaviour of χ_δ as $\Lambda \rightarrow 0$. In this limit,

$$\chi_\delta \sim \frac{\delta}{M\lambda^2}. \quad (10)$$

Assuming that the effect of the slip velocity \hat{U} on the bulk velocity in the channel $q\chi_t$ is negligibly small when $\delta \rightarrow 0$ [19, Fig.1(a)], we employ the *log-law* and the velocity-defect law of turbulent flow in a channel of width $2L$ to provide an estimate for χ_t . These two laws combined relate the friction velocity \hat{u}_τ to the channel bulk velocity $q\chi_t$,

$$\frac{1}{\kappa} + \frac{q\chi_t}{\hat{u}_\tau} = \frac{\ln Re_\tau}{\kappa} + 5.1, \quad (11)$$

where $\kappa = 0.41$ is the von Kármán constant. Inserting (6) in (11), we obtain

$$\chi_t(Re_\tau) = \frac{\ln Re_\tau + 5.1\kappa - 1}{\kappa Re_\tau}, \quad (12)$$

since $\hat{u}_\tau = \nu Re_\tau / L$. Combining (7), (8), (10) and (12) we obtain a closed form expression for the skin friction coefficient in terms of the viscosity ratio between the fluids inside and over the patterns, M , Kármán number, Re_τ , and the pattern height and effective permeability, δ and λ , respectively,

$$C_f = C_f^s \left(\frac{2 + \delta}{2 + \mathcal{T}\delta} \right)^2 \quad (13a)$$

with

$$\mathcal{T} = \frac{1}{M\lambda^2\chi_t(Re_\tau)}, \quad C_f^s = 2 \left(\frac{\kappa}{\ln Re_\tau + 5.1\kappa - 1} \right)^2. \quad (13b)$$

Here C_f^s represents the skin friction coefficient in a channel with smooth walls. Similarly, for two patterned walls, the skin friction coefficient, C_{f2} , is

$$C_{f2} = C_f^s \left(\frac{1 + \delta}{1 + \mathcal{T}\delta} \right)^2. \quad (14)$$

The turbulent drag reduction $R_D^\% = (1 - C_f/C_f^s)\%$ for a channel with one (or two) superhydrophobic walls can be readily calculated from (13a) (or (14)):

$$R_D^\% = 100 - \left(\frac{2 + \delta}{2 + \mathcal{T}\delta} \right)^2 \%. \quad (15)$$

Equations (13) and (14) provide closed-form expressions for C_f whenever the effective permeability of the micro pattern, the geometry of the channel and the operational flow conditions are known.

Comparison with experiments. – We test the robustness of our model by comparing it with experiments [7]. Data sets collected by Ref. [7, Figs. 8 and 9] include measurements of skin friction and drag reduction coefficients, C_f and $R_D^\%$ respectively, as a function of Reynolds number ($Re = 2L\hat{u}_b/\nu$) from channels with smooth walls, and one and two superhydrophobic walls containing $30\mu\text{m}$ wide microridges spaced $30\mu\text{m}$ apart. A set of dimensional and dimensionless parameters for the experiments are listed in table 1. The data span almost one order-of-magnitude wide range of Reynolds number both in laminar and turbulent regimes, $Re \in (2000, 10000)$.

A comparison between model and experiments requires one to establish a relationship between Re and Re_τ . Combining (6) with the definition of dimensionless bulk velocity χ (i.e. $q = \hat{u}_b\chi^{-1}$), and multiplying both sides by $2L/\nu$ leads to

$$Re = 2\chi Re_\tau^2. \quad (16)$$

For turbulent smooth-channel flows, combining (12) with (16) leads to a relation between Re and Re_τ in the form $Re = 2Re_\tau(\kappa^{-1} \ln Re_\tau + 5.1 - \kappa^{-1})$. Similarly, for a channel with one (or two) micro-patterned surfaces, inserting

(8) into (16) leads to $Re = 2Re_\tau^2(2 + \delta)^{-1}(\chi_\delta + 2\chi_t)$ (or $Re = 2Re_\tau^2(1 + \delta)^{-1}(\chi_\delta + \chi_t)$). Since $\chi_\delta \ll \chi_t$ as $\delta \rightarrow 0$, a good approximation of the former equations is $Re_\tau \approx 0.09Re^{0.88}$ for $Re < 4 \cdot 10^4$. Additionally, in laminar smooth-channel flows the dimensionless parabolic velocity profile, $u(y) = -y^2 + y$, $y \in [0, 2]$, gives $\chi = 1/3$. When combined with (7) and (16), this leads to the well-known skin friction formula $C_f = 12/Re$ or, equivalently, $C_f = 18/Re_\tau^2$. The former relationships allow us to rescale the data points from [7] as showed in Fig. 1. Transitional effects from laminar to turbulent regimes are apparent in the range $Re_\tau \in [100, 150]$ for channel flow with two superhydrophobic surfaces.

Except for relatively simple configurations (e.g. an array of pillars [12]), there exist no exact closed-form expressions that relate the dimensionless effective permeability λ to the geometrical properties of riblets. Therefore, we validate the proposed model by employing two sets of independent measurements from [7]. The first dataset consists of measurements of the skin friction coefficient C_f in a channel with two micro-patterned walls, for the fully turbulent regime represented by a range of Kármán number $Re_\tau \in [150, 200]$ (see the dash-lined box in fig. 1). Fitting to these data yields the value of permeability $\lambda = 4.54$. This value is used to make fit-free predictions of the skin friction coefficient C_f in a channel with one smooth wall and one micro-patterned wall, for the fully turbulent regime represented by a range of Kármán number $Re_\tau \in [100, 300]$. Figure 1, which compares this prediction (bold solid line) with the corresponding C_f measurements (filled dots) comprising the second dataset, shows a good agreement between data and model solution.

The fitted value of λ corresponds to the permeability $K = 1.8 \cdot 10^{-5} \text{m}^2$ of the effective porous medium used to represent the two $30\mu\text{m}$ -ridged superhydrophobic walls. An order-of-magnitude analysis of the permeability of this porous medium is obtained from Darcy's law, which states that the Darcy flux \hat{q}_d (volumetric flow rate per unit height H) is proportional to $|d_{\hat{x}}\hat{p}|$, the applied pressure gradient, such that

$$K = \frac{\mu_e}{|d_{\hat{x}}\hat{p}|} \hat{q}_d. \quad (17)$$

Each patterned surface in the experimental setup [7] is 38.1mm wide, consisting of an array of $n \approx 635$ square ridges of height $H = 30 \mu\text{m}$ spaced $30 \mu\text{m}$ apart. We approximate the flow between any two ridges with a fully-developed pressure-driven flow between two parallel plates the distance H apart; the bottom plate is fixed while the upper plate moves with a uniform speed $\hat{U}^* = (1 - \phi_s)^{-1}\hat{U}$ where \hat{U} is the slip velocity measured in [7] and $\phi_s = 0.5$ is the solid fraction of the patterned surface. Then $\hat{q}_d = \hat{U}^*/2 - H^2 d_{\hat{x}}\hat{p}/\mu_e$, and (17) gives the permeability of an individual channel $K_i = -\mu_e \hat{U}^*/(2d_{\hat{x}}\hat{p}) + H^2/12$ ($i = 1, \dots, n$). The total permeability of the two patterned surfaces is $K = 2 \sum_{i=1}^n K_i$.

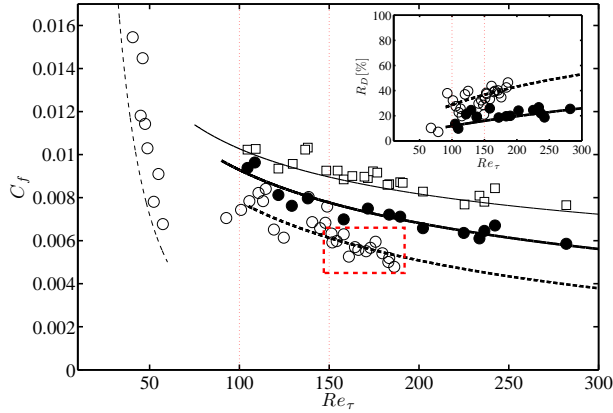


Fig. 1: Experimental (symbols) and predicted (lines) skin friction C_f in terms of Re_τ . Data adapted from [7, Fig.8]. Measurements of skin friction coefficient for a channel with smooth walls (empty squares), one (filled circles) and two (empty circles) SHS with $30\mu\text{m}$ ridges spaced $30\mu\text{m}$ apart. The thin dashed and solid lines represent the theoretical prediction of the skin friction coefficient for smooth channel, C_f^s , in laminar and turbulent regimes given by $C_f^s = 18/Re_\tau^2$ and (13b), respectively. The thick dashed and solid lines represent a one-parameter fit ($\lambda = 4.54$) and a parameter-free prediction of C_f given by (14) and (13a), respectively. The dashed box contains the data used for the parametric fitting. Inset: Experimental (symbols) and predicted (lines) drag reduction in terms of Re_τ . Data adapted from [7, Fig.9].

In [7, Fig.5b], the slip velocity $\hat{U} = 0.2 \text{ ms}^{-1}$ is reported for the channel with two patterned walls (square ridges of $H = 30 \mu\text{m}$) and $Re = 7930$. In the absence of reported pressure measurements for this channel configuration, we employ the pressure drop data reported for two other channels [7, Fig.6]. In the first channel (two smooth walls) the pressure drop was $|\text{d}_{\hat{x}}\hat{p}| = 2.6 \text{ kPa}\cdot\text{m}^{-1}$. In the second (both surfaces patterned with $H = 60\mu\text{m}$ square ridges) it was $|\text{d}_{\hat{x}}\hat{p}| = 1.4 \text{ kPa}\cdot\text{m}^{-1}$. Using these two values as upper and lower bounds for the actual $|\text{d}_{\hat{x}}\hat{p}|$, we obtain permeability bounds $1.8 \cdot 10^{-6} \text{ m}^2 \leq K \leq 3.3 \cdot 10^{-6} \text{ m}^2$. These estimates differ by a factor of 5 – 10 from the fitted value of $K = 1.8 \cdot 10^{-5} \text{ m}^2$. The discrepancy between the two is to be expected due to deviations of the experiment from the model approximations and/or highly idealised conditions, which include, e.g., flow steadiness and one-dimensionality, and hydrodynamically smoothness of the ridges’ tips.

Next, we discuss some implications of the former model. Equation (13a) implies that $C_f < C_f^s$ if $\mathcal{T} > 1$, or

$$C_f < C_f^s \quad \text{if} \quad \chi_t^{-1}(Re_\tau) > M\lambda^2, \quad (18)$$

with χ_t defined by (12) and $Re_\tau > Re_\tau^t$, with Re_τ^t the transition Kármán number between laminar and turbulent regimes. For channel flow, $Re_\tau^t \approx 100$ (or $Re^t \approx 3000$). At any fixed Kármán number, the skin

Table 1: Parameter values used in the experiments of [7] with channels with smooth walls, one and two superhydrophobic surfaces with $30\mu\text{m}$ ridges spaced $30\mu\text{m}$ apart. Dimensionless quantities are calculated from corresponding dimensional parameters.

Sample	Smooth	1 SHS	2 SHS
L [m]	$3.95 \cdot 10^{-3}$	$3.95 \cdot 10^{-3}$	$2.75 \cdot 10^{-3}$
H [m]	0	$25 \cdot 10^{-6}$	$25 \cdot 10^{-6}$
μ [Pa·s]	$8.90 \cdot 10^{-4}$	$8.90 \cdot 10^{-4}$	$8.90 \cdot 10^{-4}$
μ_e [Pa·s]	$8.90 \cdot 10^{-4}$	$1.78 \cdot 10^{-5}$	$1.78 \cdot 10^{-5}$
δ [-]	0	$6.33 \cdot 10^{-3}$	$9.01 \cdot 10^{-3}$
M [-]	1	0.02	0.02

friction C_f is smaller than its smooth channel counterpart when appropriate conditions of the roughness/pattern geometry, λ and δ , and of the fluids, M , are met. Also, since $\chi_t^{-1}(Re_\tau)$ is a convex function, (18) implies the following:

Proposition. For any fixed configuration of obstacles, λ , and fluid viscosity ratio, M , such that $M\lambda^2 \geq \chi_t^{-1}(Re_\tau^t) \approx 7.2$, there exists a critical Kármán number, Re_τ^* , such that $C_f \leq C_f^s$ if $Re_\tau > Re_\tau^*$ where Re_τ^* is a root of the transcendental equation

$$\kappa Re_\tau^* (\ln Re_\tau^* + 5.1\kappa - 1)^{-1} = M\lambda^2, \quad Re_\tau^* > Re_\tau^t. \quad (19)$$

The existence of a Re_τ^* is consistent with experimental results, where drag reduction is initiated at a critical Reynolds number, just past the transition to turbulent flow [7]. The former statement can be reformulated as a condition on the geometrical properties of the patterns/roughness, λ , and the viscosity ratio, M : for any fixed value of Kármán number $Re_\tau^0 > Re_\tau^t$, drag reduction is achieved if the product $M\lambda^2$ is bounded from below and above, i.e.

$$\chi_t^{-1}(Re_\tau^t) < M\lambda^2 < \chi_t^{-1}(Re_\tau^0), \quad Re_\tau^0 > Re_\tau^t \quad (20)$$

with χ_t defined in (12), and $\chi_t^{-1}(Re_\tau^t) \approx 7.2$.

This analysis has the following implications. (i) The proposed model suggests that drag reduction is achieved when $\lambda > 1$, i.e. in the *porous medium* regime [13], and for an intermediate range of effective permeability values. The upper bound on λ (i.e. the minimum value of permeability) is determined by the magnitude of Re_τ^0 , i.e. the operational flow conditions of the apparatus/system. This is consistent with passive turbulent flow control systems where porous surfaces in airfoils are employed for drag reduction purposes. (ii) The transition between drag enhancing and reducing regimes is governed by the geometric parameters of the obstacles, λ , and the viscosity of the fluid flowing between the roughness/pattern and above

it, M. (iii) For any fixed geometry and $Re_\tau > Re_\tau^*$, lower drag is achieved in Cassie/Fakir state than in Wenzel state since $M < 1$ in the former case. Also this result is consistent with experimental observations. While the former observations are qualitatively consistent with experiments, future work will focus on a quantitative analysis/estimate of each process above mentioned.

Concluding remarks. – We proposed a novel continuum-scale framework to modelling turbulent flows over micro-patterned surfaces. While applicable to flows over patterned surfaces both in Cassie and Wenzel state, we test the model on turbulent flows over superhydrophobic ridged surfaces. To the best of our knowledge, this is the first continuum-scale framework that allows one to successfully quantify and analytically predict the impact of pattern geometry and Reynolds number on drag reduction. This is achieved by modelling the micro-patterned surface as a porous medium, and by coupling Brinkman equation for flow in porous media with Reynolds equations, which describe the average flow through and over the pattern, respectively. This yields a closed-form solution for the skin friction coefficient in terms of the frictional Reynolds (Kármán) number, the viscosity ratio between the outer and inner fluid, and the geometrical (i.e. height) and effective properties (i.e. permeability) of the micro-structure. We demonstrated good agreement between our model and experimental data.

Based on dynamical and geometrical conditions under which the proposed model predicts drag reduction, we conjecture that the latter might be attributed to a *porous-like* medium behaviour of the roughness/pattern. We speculate that our results might provide an insight on the transition between turbulent flows over drag-increasing [20] and drag-decreasing rough walls where patterned protrusions, rigid or compliant [6,21] to the flow, or porous coatings [22], can be used to attenuate near wall turbulence. Yet, the connection between the flow characteristics at the pattern-scale and their effective-medium behaviour needs to be elucidated and is subject of current investigations.

Part of this research was developed when the author was first a postdoctoral fellow at Max Planck Institute for Dynamics and Self-Organization (MPI-DS), Göttingen, 37077, Germany, and later a visiting scientist at the Statistical and Applied Mathematical Sciences Institute (SAMSI), Research Triangle Park, NC 27709, USA.

REFERENCES

- [1] COTTIN-BIZONNE C., BARRAT J.-L., BOCQUET L. and CHARLAIX E., *Nat Mater*, **2** (2003) 237.
- [2] JOSEPH P., COTTIN-BIZONNE C., BENOIT J.-M., YBERT C., JOURNET C., TABELING P. and BOCQUET L., *Phys Rev Lett*, **97** (2006) 156104.
- [3] CHOI C.-H., ULMANELLA U. and KIM J., *Phys Fluids*, **18** (2006) 087105.
- [4] YBERT C., BARENTIN C., COTTIN-BIZONNE C., JOSEPH P. and BOCQUET L., *Phys Fluids*, **19** (2007) .
- [5] LEE C., CHOI C.-H. and KIM C.-J., *Phys Rev Lett*, **101** (2008) 064501.
- [6] SIROVICH L. and KARLSSON S., *Nature*, **388** (1997) 753.
- [7] DANIELLO R. J., WATERHOUSE N. E. and ROTHSTEIN J. P., *Phys Fluids*, **21** (2009) .
- [8] ROTHSTEIN J. P., *Ann Rev Fluid Mech*, **42** (2010) 89.
- [9] LAUGA E. and STONE H. A., *J Fluid Mech*, **489** (2003) 55.
- [10] DAVIS A. M. J. and LAUGA E., *J Fluid Mech*, **661** (2010) 402.
- [11] BOUCQUET L. and LAUGA E., *Nature Mater*, **10** (2011) 334.
- [12] BATTIATO I., BANDARU P. R. and TARTAKOVSKY D. M., *Phys Rev Lett*, **105** (2010) 144504.
- [13] BATTIATO I., *J Fluid Mech*, **699** (2012) 94.
- [14] OCHOA-TAPIA J. and WHITAKER S., *Intl J. Heat Mass Transfer*, **38** (1995) 2635.
- [15] CIESZKO M. and KUBIK J., *Transport in Porous Media*, **34** (1999) 319.
- [16] JÄGER W. and MIKELIĆ A., *SIAM J. Appl. Math.*, **60** (2000) 1111.
- [17] WEINBAUM S., ZHANG X., HAN Y., VINK H. and COWIN S. C., *PNAS*, **100** (2003) 7988.
- [18] BARS M. L. and WORSTER M. G., *J. Fluid Mech.*, **550** (2006) 149.
- [19] FUKAGATA K., KASAGI N. and KOUMOUTSAKOS P., *Phys. Fluids*, **18** (2006) .
- [20] CASTRO I., *J. Fluid Mech.*, **585** (2007) 469.
- [21] BRÜCHER C., *J. Phys.: Condens. Matter*, **184120** (2011) 1.
- [22] VENKATARAMAN D. and BOTTARO A., *Phys. Fluids*, **24** (2012) .